Nuclear magnetic resonance study of Li implanted in a thin film of niobium

T. J. Parolin,[1] J. Shi,[1] Z. Salman,[2,*] K. H. Chow,[3] P. Dosanjh,[4] H. Saadaoui,[4] Q. Song,[4] M. D. Hossain,[4] R. F. Kiefl,[2,4,5] C. D. P. Levy,[2] M. R. Pearson,[2] and W. A. MacFarlane[1]

[1]*Chemistry Department, University of British Columbia, Vancouver, British Columbia, Canada V6T 1Z1*

[2]*TRIUMF, 4004 Wesbrook Mall, Vancouver, British Columbia, Canada V6T 2A3*

[3]*Department of Physics, University of Alberta, Edmonton, Alberta, Canada T6G 2G7*

[4]*Department of Physics and Astronomy, University of British Columbia, Vancouver, British Columbia, Canada V6T 1Z1*

[5]*Canadian Institute for Advanced Research, Toronto, Ontario, Canada M5G 1Z8*

(Received 30 July 2009; revised manuscript received 29 September 2009; published 13 November 2009)

We report results of beta-detected NMR of $^8Li^+$ implanted in Nb at high magnetic field. We identify two distinct sites for ^8Li in the body-centered lattice. At low temperature, the site is characterized by a well-defined quadrupolar splitting. At about 50 K this site becomes unstable. Close to room temperature, Li occupies the cubic substitutional site. Spin-lattice relaxation measurements are consistent with a site-dependent coupling to the Nb conduction electrons and suggest that the site change proceeds in two steps. We report Knight shifts for the two well-defined sites and perform a Korringa analysis.

DOI: 10.1103/PhysRevB.80.174109 PACS number(s): 61.72.−y, 74.62.Dh, 76.60.−k, 74.25.Ha

I. INTRODUCTION

Niobium is the highest transition-temperature elemental superconductor (T_C=9.3 K). Its structural simplicity and many decades of detailed study make it one of the best understood conventional superconductors; however, important refinements continue to be made.[1] The superconductivity of Nb finds current application in, for example, radiofrequency (RF) particle accelerators.[2] For the highest Q-factor cavities, particular attention must be paid to the surface preparation, and the occurrence of surface and interstitial oxides,[3] some of which are also superconducting.[4] Additionally, Nb is widely studied as a superconducting layer in thin film heterostructures involving normal metals[5] or semiconductors,[6] which exhibit many fascinating properties.

In the context of thin films, it would be valuable to have a local probe such as nuclear magnetic resonance (NMR) to obtain a spatially resolved measurement of the electronic structure. NMR in thin films is, however, hampered by the small number of nuclei (and therefore small signal), and only a few such studies have been undertaken.[7] Recently we have developed instruments based on the related technique of beta-detected NMR (β-NMR), using a low-energy beam of radioactive probe ions introduced into solids in a depth-controlled manner.[8,9] In order to interpret measurements on heterostructures[10] and to establish the technique, we have studied face-centered cubic (fcc) elemental metals.[8,11–13] In the current work we use the implanted hyperpolarized beam of ^8Li to study a thin film of body-centered cubic (bcc) Nb. We present both resonance and spin-lattice relaxation (T_1) data for ^8Li in the normal state of Nb in two different samples. From the resonance spectra, we find the stopping site for Li changes below about 70 K. We measure the Knight shift of the implanted Li as well as the temperature dependence of $1/T_1$, which is not simply Korringa-like. We discuss the results in terms of the lattice location of the implanted Li and compare with the fcc metals.

II. EXPERIMENT

We present data on a 15 micron foil of 99.9% Nb (Goodfellow) and a 300 nm thick film. The film was deposited at 1 Å/s by RF sputtering onto an epitaxially polished sapphire ⟨0001⟩ substrate (Honeywell) at ~50 °C in 3 mTorr of Argon (flowing at 25 SCCM) using a 99.9% Nb target (Goodfellow). The base pressure of the sputtering chamber was 2×10^{-7} Torr and the target was presputtered for an hour before deposition. X-ray diffraction showed that the film was very highly oriented in the ⟨110⟩ direction with a typical rocking curve width of 1°. X-ray pole figure analysis further reveals significant in plane orientation consistent with another report of low-temperature Nb growth on c-plane sapphire.[14] This is in contrast to epitaxial growth of Nb at higher temperature, where the ⟨111⟩ orientation is the most stable.[14,15] Similar measurements on the foil showed no significant orientation.

The experiments were conducted at the TRIUMF ISAC facility, which provides a low energy (<30 keV) beam of highly spin-polarized $^8Li^+$ with a flux of $\sim10^6$ ions/s in a beam spot ~3 mm in diameter. The spin polarization, typically ≃70%, is produced in-flight by optical pumping.[16] By selecting the sense of circular polarization (helicity) of the pump laser, one selects the spin-polarization direction either parallel or antiparallel to the applied magnetic field. Both polarizations are collected alternately to reduce systematics and to give an accurate baseline. The two helicities are usually combined before analysis, but sometimes it is useful to consider them separately. The probe ^8Li has nuclear spin I =2, gyromagnetic ratio γ=6.3015 MHz/T, lifetime τ =1.21 s and quadrupole moment Q=+31.4(2) mb.[17] From simulations using SRIM2006.02,[18] the 30 keV implantation energy corresponds to a mean implantation depth of 94 nm (with a distribution width of 44 nm) for the $^8Li^+$ ions in the 300 nm Nb/Al_2O_3, i.e., none of the $^8Li^+$ will penetrate the film to reach the substrate.

The $^8Li^+$ is implanted into the sample which is held in a static external field (H_0) parallel to the beam (normal to the sample surface). For these measurements, $H_0 \gg H_{c2}$, the upper critical field for superconductivity, so all the results are in the normal state of Nb. The samples were mounted on a helium cold finger cryostat in an ultrahigh vacuum chamber

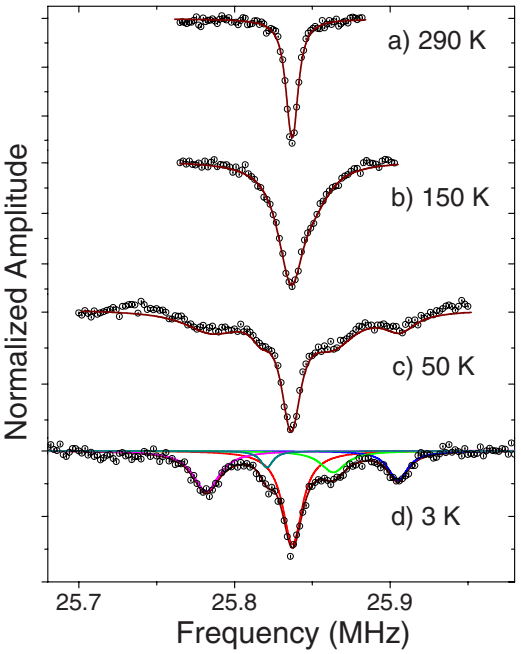

FIG. 1. (Color online). Representative β-NMR spectra with Lorentzian fits of ^{8}Li in Nb (oriented film) with H_0=4.1 T. (a) At room temperature a single resonance from the substitutional sites is observed ($H_1 \approx 10$ μT). (b) The broadened resonance at 150 K appears to contain an additional unresolved resonance. (c) For $T < 70$ K, a quadrupole split resonance due to the noncubic interstitial site appears, becoming better resolved at lower temperature. For (b)–(d), $H_1 \approx 40$ μT.

($\sim 10^{-9}$ Torr). High energy beta electrons from the decay of ^{8}Li are detected in two fast plastic scintillation detectors upstream (backward, B) and downstream (forward, F) of the sample. The count rates are combined to generate the asymmetry $A=(F-B)/(F+B)$ which through the properties of the beta decay is proportional to the ^{8}Li nuclear spin polarization $P=(\Sigma_m m P_m)/I$, where m is the magnetic quantum number and P_m is the population of the corresponding magnetic sublevel with quantization axis defined by H_0. To measure the spin resonances, a small RF field H_1 is applied perpendicular to the polarization. On resonance, the continuous wave RF causes the ^{8}Li spins to precess rapidly compared to the integration time, effectively destroying the polarization, so that the signal appears as a *loss* of asymmetry. Here we measure the resonance with a continuous beam of ^{8}Li and step the frequency slowly compared to $\Delta\nu/\tau$, where $\Delta\nu$ is the resonance linewidth. In this regime, the signal is the intrinsic line convoluted with a power broadening Lorentzian $f(\nu) = \gamma H_1/(\nu^2+\gamma^2 H_1^2)$.

The spin-lattice relaxation rate $\lambda = 1/T_1$ is measured (in the absence of H_1) by pulsing the incident ion beam with an electrostatic kicker and measuring the time dependence of A after each pulse. We used a 500 ms beam pulse, followed by a counting period of 10 s. Decay events were accumulated by repeating this cycle for an average of 30 minutes per temperature. For the case of a simple single exponential relaxation, the asymmetry after the beam pulse δ follows:

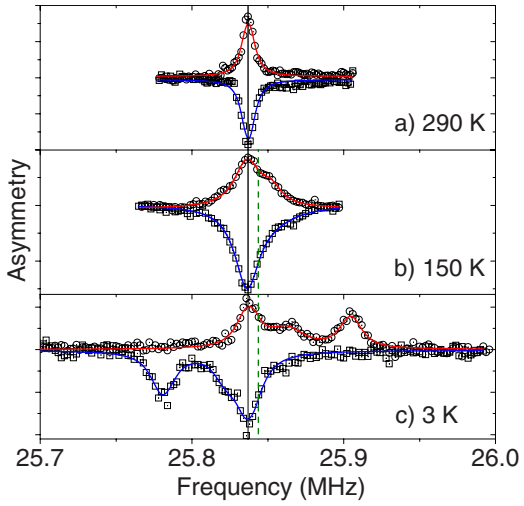

FIG. 2. (Color online) Resonances in the film for ^{8}Li polarized parallel and antiparallel to H_0. (a) The spectrum at 290 K shows no quadrupolar splitting. (b) At 150 K, the line is broader and one helicity has a high-frequency shoulder. (c) At low temperature the quadrupolar splitting of the interstitial site is clearly revealed as satellites on opposite sides of the Larmor frequency for opposite helicities. The solid vertical line marks the resonance position at high temperature, while the dashed line is the center of mass of the outer satellites.

$$A = A_\delta e^{-(t-\delta)\lambda}, \tag{1}$$

where A_δ is the asymmetry at the trailing edge of the pulse. For the spin relaxation in Nb, a single exponential provided a good fit to the data.

III. RESULTS AND DISCUSSION

Frequency spectra were collected in the film over the temperature range 3–300 K in a magnetic field of 4.1 T. Representative data, fit with a sum of Lorentzians, are shown in Fig. 1. At room temperature, a single line about 9 kHz broad [full width at half maximum (FWHM)] is observed near the Larmor frequency. This is similar to what is seen in Ag (Ref. 8) and Au;[11,19] however, the line is substantially broader for Nb. The absence of quadrupolar splitting of the line indicates that Li is at a site of cubic symmetry with vanishing electric field gradient (EFG). Further evidence for the absence of quadrupolar effects comes from a comparison of the spectra with opposite helicity, see Fig. 2 (top). If there were a distribution of small (a few kHz) quadrupole splittings, one would find resonances in the opposite helicity channels to be asymmetric and skewed in the opposite direction. At room temperature, this implies ^{8}Li is located at the only cubic site in the Nb lattice, i.e., the substitutional (S) site. As the temperature is reduced, however, the resonance broadens substantially then, below 70 K, changes dramatically to include a set of quadrupole satellites in addition to the original main line [Figs. 1 and 2(c)]. Thus at low temperature, a fraction of the ^{8}Li stops in a site of less than cubic symmetry, most likely an interstitial (I) site.

Ions implanted into solids typically occupy high-symmetry sites in the host lattice which represent a local

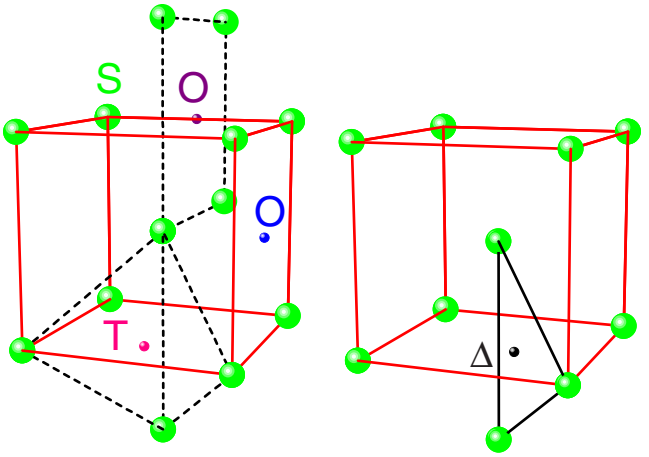

FIG. 3. (Color online) The bcc unit cell of Nb, indicating the high-symmetry interstitial sites and the substitutional (S) site. The face center and edge center are equivalent and are at the center of a distorted octahedron (O). A representative $\mathcal{T}$ site is the center of the dashed quasitetrahedron at $(\frac{1}{4},\frac{1}{2},0)$ In the right panel a trigonal interstitial site (Δ) is shown. It is equidistant from three near neighbors at the vertices of the isosceles triangle at $(\frac{3}{8},\frac{5}{8},0)$. The lattice constant a=3.30 Å, so the near neighbor distances are 1.65 Å (O), 2.86 Å (S), 1.84 Å ($\mathcal{T}$), and 1.75 Å (Δ).

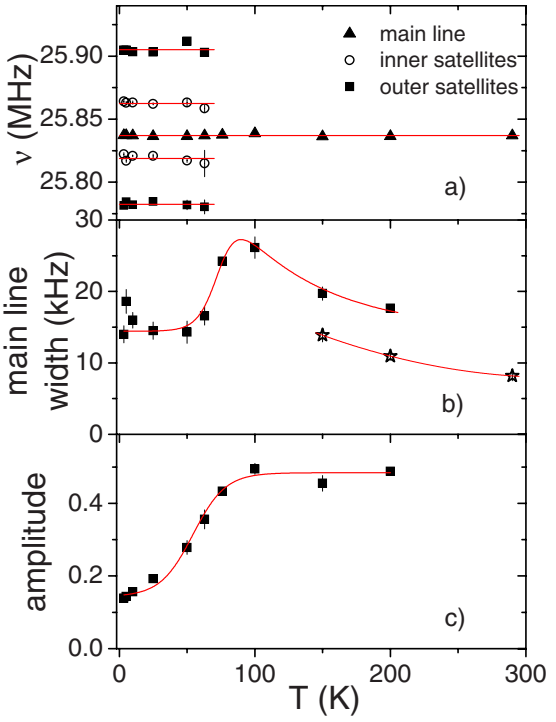

FIG. 4. (Color online) (a) Resonance frequencies as a function of temperature: main line (filled triangles); outer quadrupole satellites (filled squares); inner satellites (open circles). (b) Main linewidth (FWHM) and (c) normalized amplitudes, of the main line. In (b) the stars are data taken at lower power $H_1 \approx 10$ μT (less power broadened) and indicate the narrowing trend continues to room temperature. Lines are guides to the eye.

electrostatic potential minimum. The value of the quadrupolar splitting in high magnetic field is determined by the product of the EFG at the nucleus q and the nuclear electric quadrupole moment Q. ^{8}Li's small Q yields small quadrupole splittings typically in the range of 10–100 kHz in insulators.[20,21] Interestingly, the splitting in Nb (~50 kHz) is also on this order. This measurement of the EFG will provide an important test for modern calculations of hyperfine interactions in metals.[22]

In bcc Nb, there are several candidate I sites (see Fig. 3).[23] The face center and edge center of the conventional cubic unit cell are equivalent sites of quasioctahedral coordination (denoted O hereafter), with two near neighbors at $a/2$ and four at $\sqrt{2}a/2$. Midway between each face center and each edge center is a quasitetrahedral ($\mathcal{T}$) site with four neighbors at $\sqrt{5}a/4$. In addition, there is a trigonal (Δ) site equidistant from an isosceles triangle of three near neighbors at $3\sqrt{2}a/8$. While the first two sites have been considered for light implanted ions in bcc metals,[24,25] the latter has not. The Δ site is, however, known to be an important Ag^+ site in the superionic conductor α-AgI.[26] This is in contrast to the fcc metals Ag and Au,[8,11,19] where both the interstitial and substitutional sites are cubic, and the resonances are only distinguished by their Knight shifts. Previous studies[27,28] involving cubic metals and second period impurity atoms (e.g., ^{12}B and ^{12}N), have concluded that the larger octahedral interstitial sites are favored over the tetrahedral ones. For the bcc lattice, the near neighbor distance in the $\mathcal{T}$ site is larger than the O site and Δ is intermediate. Consistent with the more spacious $\mathcal{T}$ site, β-NMR studies of ^{12}B in bcc vanadium conclude a significant fraction of implanted ^{12}B occupies a substantially expanded $\mathcal{T}$ site,[24] based primarily on a static dipolar line broadening interpretation. Later cross-relaxation measurements of ^{12}B in V agreed broadly but revised this site assignment to the O site.[25] In neither case was the site occupation investigated systematically as a function of temperature.

One contribution to the resonance broadening is the host lattice nuclear magnetic dipoles. For Nb, the moments (100% ^{93}Nb with γ=10.45 MHz/T) are much larger than Ag or Au. The dipolar linewidth depends on both the direction of the applied field in the crystal lattice and the probe site. Calculations of the dipolar width (FWHM) for the Nb lattice and the candidate sites yield values for $H_0 \| \langle 110 \rangle$ of 4.1 kHz (S), 5.3 kHz (O), 10.2 kHz ($\mathcal{T}$), and 6.8 kHz (Δ). We note these values are substantially smaller than the observed width; which is, moreover, significantly temperature dependent, implying another source of broadening is important. It is, thus, not possible to infer the site on the basis of the linewidth.

The temperature dependence of the resonance spectra of ^{8}Li in Nb is summarized in Fig. 4. The resonance positions are independent of temperature, both for the S and I lines. With increasing T, the interstitial lines first broaden [see Fig. 1(c)], then disappear above about 70 K, where the S line broadens substantially. From Fig. 4(c), there is a substantial increase in the amplitude of the S line from 50 to 100 K, which is qualitatively consistent with the loss of amplitude in the I lines. However, a small shoulder at higher frequency [Figs. 1(b) and 2(b)] may be an unresolved remnant of the I resonance.

The quadrupolar splitting also contains site information. The scale of the quadrupolar interaction is the quadrupole

frequency ν_Q, which for ^{8}Li is $e^2qQ/4h$, where q is the EFG at the nucleus, e the electron charge, and h Planck's constant. ν_Q sets the scale for the splitting, i.e., a few 10s of kHz, thus $\nu_Q/\nu_0 \sim 0.002$, and the quadrupolar interaction can be treated as a first-order perturbation on the Zeeman interaction. For both the O and $\mathcal{T}$ sites, the EFG is axially symmetric, and the transition frequencies are

$$\nu[m \leftrightarrow m-1] = \nu_0 - \frac{\nu_Q}{2}\left(m - \frac{1}{2}\right)[3\cos^2\theta - 1], \qquad (2)$$

where $m=-1\cdots 2$, and θ is the angle between the applied magnetic field and the symmetry axis of the EFG tensor.[29] Due to the high polarization of the ^{8}Li nuclei, predominantly the $m=2$ (-2 for the opposite helicity) state is populated initially, so we expect only the outermost satellite transition $2\leftrightarrow 1(-2\leftrightarrow -1)$ to be evident in the spectrum as was seen in, e.g., $SrTiO_3$.[21]

By symmetry, for both O and $\mathcal{T}$ sites, the principal z axis of the EFG is along a $\langle 100\rangle$ direction.[25] The applied field in the $\langle 110\rangle$ direction breaks the symmetry, yielding two angles $\theta=45°$ and 90° in a 2:1 intensity ratio. Thus the factor $[3\cos^2\theta - 1]=+0.5$ and -1, implying that there should be satellites *on both sides* of ν_0 in each helicity. In contrast, the data [Fig. 2(c)] show satellites only on *one* side of ν_0 in each helicity. This is also in contrast to the β-NMR spectrum of ^{12}B in V, which shows large outer satellite transitions on both sides of ν_0, consistent with the O-site assignment.[25] The spectrum in Fig. 2(c) thus rules out these sites for ^{8}Li in Nb, and we must consider other possibilities.

For the Δ site, the EFG is *nonaxial*, i.e., the EFG asymmetry parameter η is nonzero.[29] However, because it lies at the intersection of two orthogonal mirror planes of the crystal, the principal axes are directed along $\langle 110\rangle$, $\langle 1\bar{1}0\rangle$, and $\langle 001\rangle$. For any choice of these as the EFG's z axis, the nonaxial analog[30] of Eq. (2) yields three distinct combinations of angles corresponding to three distinct lines for the $2\leftrightarrow 1$ (or $-2\leftrightarrow -1$) transition, with 2 on one side of ν_0 and 1 on the other. This is inconsistent with the observed spectrum, and so we also rule out this site.

The quadrupole satellites are, however, quite well defined. For the 3 K spectrum the linewidth of the resolved satellite is ~20 kHz, while the central line is ~15 kHz wide (FWHM). The small excess broadening of the satellite has some contribution from a distribution of angles, since the film is not perfectly oriented. The well-resolved spectrum implies a well-defined local environment for the interstitial; although none of the interstitial sites considered so far can account for it. In many metals, channeling studies[31] find that solute atoms form mixed (split) interstitial "dumbell" configurations, where a bound solute-atom—host-atom pair straddle a lattice site, with the solute atom consequently displaced significantly from the high-symmetry site. This interstitial complex has been discussed theoretically[32] and invoked to explain high interstitial mobility in bcc lattices.[33] Although we have not observed the corresponding quadrupolar splitting of the analogous configuration in the fcc metals, it must be considered a possibility here. The axis of mixed dumbells in a bcc lattice generally lies along a $\langle 110\rangle$ direction, i.e., it corresponds to a distorted Δ site. Alternatively, the site could represent the heteroatom analogue of the $\langle 111\rangle$ "crowdion" configuration of the self-interstitial,[34] as suggested for undersized solutes in Nb.[35] In pure bcc hosts, the crowdion configuration results in distinct defect dynamics, such as the low-energy barrier for long-range, one-dimensional diffusion of the self-interstitial.[36,37] Detailed calculations of the EFG for such configurations are required to determine whether they are consistent with the observed spectra. We return to a discussion of the ^{8}Li sites below.

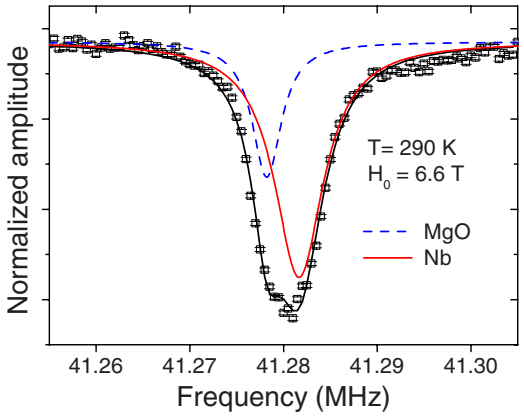

FIG. 5. (Color online). A composite spectrum of Nb and the cubic insulator MgO at 6.55 T and room temperature fit to two Lorentzians yielding the Knight shift of ^{8}Li at the S site.

We turn now to the shift of the resonance. For this measurement, the Nb foil was wrapped around a crystal of the cubic insulator MgO. ^{8}Li implanted in MgO exhibits a narrow resonance near the Larmor frequency, and we use this signal as an *in situ* field reference. Since the foil was much too thick for the $^8Li^+$ beam to penetrate, it was pierced with a pinhole onto which the beam was centered, allowing a composite spectrum to be recorded. Figure 5 shows the resonance obtained at 290 K and $H_0=6.55$ T. The asymmetric, partially resolved line was fit with two Lorentzians, the smaller one having a width typical of MgO and small amplitude consistent with the pinhole being a small fraction of the beam spot area. The larger resonance, due to Li in the S site in the Nb foil, is shifted positively by a few kHz. From this fit, the shift of ^{8}Li in the S site at 290 K is

$$K_S = \frac{\nu - \nu_{\mathrm{ref}}}{\nu_{\mathrm{ref}}} = +85(5)\ \ \mathrm{ppm}, \qquad (3)$$

where ν is the resonance frequency in Nb, and ν_{ref} is the frequency in MgO. The value is similar to the shifts of ^{8}Li in other metals.[11] To obtain the Knight shift, we must correct K_S for macroscopic demagnetization. To an excellent approximation, the thin film in perpendicular field has a geometric demagnetization factor $N=4\pi$, and the corrected shift is thus $K_S^c = K_S + \frac{8\pi}{3}\chi$, where χ is the dimensionless magnetic susceptibility in the cgs system.[38] Using a room temperature value[39] of $\chi = 20\times 10^{-6}$ (cgs), we obtain $K_S^c = +253(5)$ ppm. We note χ is slightly temperature dependent below room temperature,[39] changing by about 3% of the room-temperature value. This would yield an approximately 8 ppm

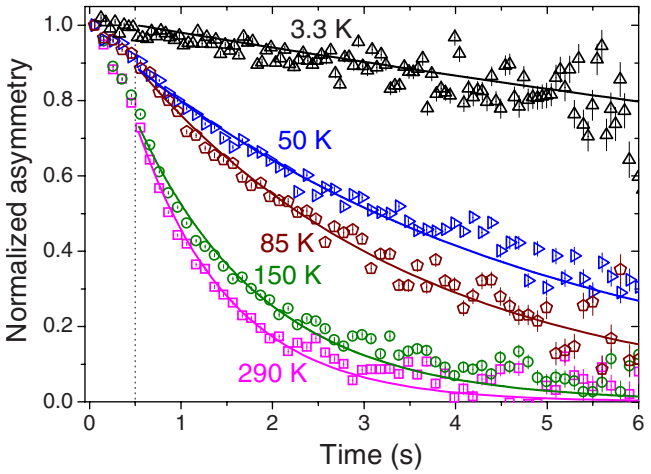

FIG. 6. (Color online) Fits of the spin relaxation in the Nb film at H_0=4.1 T for several temperatures. The dashed vertical line is the trailing edge of the beam pulse. Solid lines are fits to a single exponential relaxation.

increase in K_S^c upon cooling, which is too small to be resolved in the data, e.g., see Fig. 4.

K_S from the foil may be used to infer the shift of the interstitial ^{8}Li, K_I, in the film. We use the center of mass of the satellite lines as the resonance frequency for the interstitial. As is apparent in Fig. 4(a), the interstitial line is shifted *higher* in frequency than the *S* line, see the dashed lines in Fig. 2. We find a total shift K_I=+320(20) ppm, for a corrected value of K_I^c=+488(20) ppm at 3 K.

Measurements of the spin relaxation in the Nb film are shown in Fig. 6. The relaxation is strongly temperature dependent and well fit to a single exponential [Eq. (1)], yielding the relaxation rates λ plotted as a function of temperature in Fig. 7 and as a function of magnetic field at 10 K in Fig. 8.

In metals λ is usually dominated by the magnetic field-independent, *T*-linear Korringa relaxation due to the conduction electrons.[40] However, the observed λ(*T*) is not simply linear, but exhibits linear regimes below ~20 K and between 60 and 220 K. The dependence of λ on magnetic field at 10 K is shown in Fig. 8 and indicates that, at H_0=4.1 T, the relaxation is field independent. There is an upturn in λ below 1 T, suggesting another relaxation mechanism at low field [as found in Au (Ref. 11) and $NbSe_2$ (Ref. 41)]. This is likely due to interaction between the ^{8}Li and the dynamic host nuclear spins, but here the upturn occurs at much higher fields (about 100 times that in $NbSe_2$ at 8 K and 300 times that in Au at 290 K), implying a much stronger coupling to the host lattice spin bath.

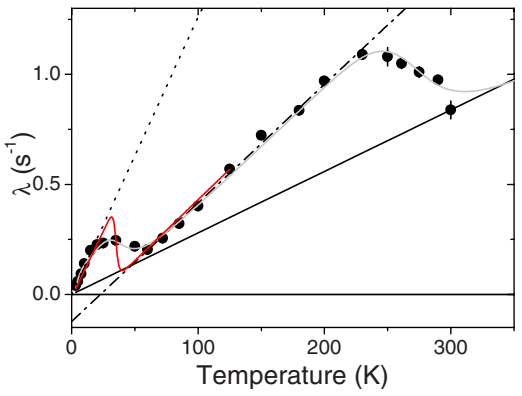

FIG. 7. (Color online) Spin-lattice relaxation rates as a function of temperature in the Nb film at H_0=4.1 T. The light curve is a guide to the eye. The linear fits are 0.01271(39) $(\mathrm{sK})^{-1}\times T$ below 20 K (dotted), 0.00554 $(\mathrm{sK})^{-1}\times T-0.138$ s^{-1} from 60 to 220 K (dot dash), and 0.0028 $(\mathrm{sK})^{-1}\times T$ (solid line), an upper limit for the slope above 300 K. The dark solid curve is a fit to the temperature dependence below 150 K using the activated site change model described in the text.

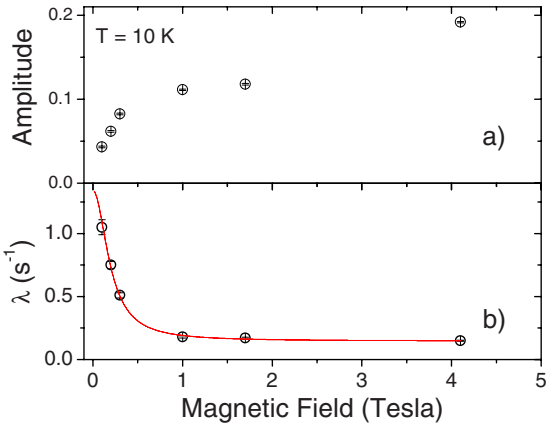

FIG. 8. (Color online) The magnetic field dependence of (a) the relaxing amplitude and (b) the spin-lattice relaxation rate from single exponential fits to relaxation data in the film at 10 K. The curve in (b) is a Lorentzian centered at zero of width 0.2 T.

The hyperfine coupling between the implanted ^{8}Li and the host conduction band depends on the site as evident in the shifts. The corresponding Korringa slope of λ(*T*) depends on the square of the coupling, so it will also be site dependent. The "peak" at about 30 K, which coincides with the onset of the disappearance of the quadrupole satellites in the resonance data, is thus a crossover from the high slope of the low-temperature metastable *I* site to the lower slope of the *S* site, as in Ag.[42] There are, however, some difficulties with this interpretation. First is the downturn in λ above 220 K which has no obvious coinciding change in the resonance (other than some narrowing). The second is that the upper linear region clearly extrapolates to a *negative* value at $T=0$ inconsistent with Korringa relaxation.

To make the analysis of λ(*T*) more quantitative, we adopt a simple activated site change model and restrict ourselves to the region below 150 K, where changes are apparent in both the resonance and relaxation data. We assume two sites with distinct exponential spin relaxation rates λ_1 and λ_2 and a site change frequency for $1\rightarrow 2$ of $\nu_{sc}=\nu_a \exp(-E_b/T)$ where E_b is the energy barrier (in K) and ν_a is an attempt frequency. Solving a simple system of linear differential equations, we find biexponential relaxation with two rates $\lambda_1+\nu_{sc}$ and λ_2. The data are, however, not significantly biexponential. So, we assume the single exponential fits represent the weighted average relaxation rate of the model, i.e., $\lambda_{obs}=f(\lambda_1+\nu_{sc})+(1-f)\lambda_2$, where the weighting factor *f* is a complicated function of the variables of the model. Lastly we assume

simple temperature dependences to each relaxation rate $\lambda_1(T)=c_1T$, i.e., a Korringa dependence. For $\lambda_2(T)$, however, we adopt an effective temperature dependence that is linear with a negative intercept (dot-dashed line in Fig. 7). The results of a least-squares fit to this model is shown as the dark solid curve in Fig. 7, where $\nu_a \sim 10^{12}$ yields a barrier of about 900 K. The main drawback of this model (which works well for a similar site change in Ag)[42] is that the activated dependence is much sharper in temperature than the data. This suggests that, rather than a single barrier for the transition, there may be a broad distribution of barriers (and possibly attempt frequencies), though the situation is likely more complex as we discuss below.

The Knight shift arises from the hyperfine interaction which, for the implanted $^8Li^+$, is a measure of the hybridization of the unoccupied $2s$ orbital with the conduction band. The hyperfine coupling constant A_{hf} is defined by

$$K^c = \frac{nA_{hf}(\chi_P/N_A)}{g\mu_B} \tag{4}$$

where n is the coordination of the Li site; χ_P is the Pauli paramagnetic spin susceptibility per Nb atom, and μ_B the Bohr magneton. Taking $\chi_P=109\times10^{-6}$ emu/mol from the Sommerfeld coefficient,[43] one obtains $A_{hf}^S=1.62(3)$ kG/μ_B for $n=8$. For the interstitial site, we do not have a definitive coordination n, so the total hyperfine coupling to the n near neighbors is $A_{hf}^I n=25(1)$ kG/μ_B. These A_{hf} values provide a stringent test of detailed calculations of the electronic structure of the isolated $^8Li^+$ in Nb.

The Korringa law relates the relaxation rate due to the conduction electrons to the square of the Knight shift; therefore, the Korringa ratio,

$$\mathcal{K} = (K^c)^2 T_1 T/\mathcal{S}, \tag{5}$$

where the constant $\mathcal{S}$, for ^{8}Li, is 1.20×10^{-5} sK. $\mathcal{K}$ is a dimensionless quantity which, for noninteracting electrons, equals 1. $\mathcal{K}$ is thus often used as a phenomenological measure of correlations, but even for rather weakly interacting electrons, it often exceeds unity,[40,43] and disorder may also play an important role.[44] Using the slope of λ below 20 K, we estimate $\mathcal{K}_I=1.5(2)$. For the substitutional site, we do not have a well determined Korringa slope, but we can still make some rough estimates of $\mathcal{K}_S$ as follows. Using the value of λ at 300 K, we can estimate an upper limit for the slope above room temperature (solid line in Fig. 7), which yields $\mathcal{K}_S \geq 1.9$. Alternatively, using the slope in the intermediate linear regime (despite the negative intercept) gives $\mathcal{K}_S \simeq 1$. One can compare these values with $\mathcal{K}=6.3$ from conventional NMR of bulk Nb.[43] As in the group 11 fcc metals, $\mathcal{K}$ from ^{8}Li β-NMR is much closer to unity than the corresponding value from NMR of the pure host.[11]

We return now to discuss the implantation sites. The transition between the two well-defined sites, the low-temperature interstitial and high-temperature substitutional, is gradual in contrast to the fcc metals.[11] The quadrupolar satellites broaden, but do not shift as temperature is increased, while the main line broadens substantially. Above 70 K, an unresolved remnant of the I resonance may contribute to the broad main line resonance [Fig. 4(a)]; Moreover, the transition in the spin-lattice relaxation appears to proceed by two steps, the first coinciding with the disappearance of the quadrupole satellites, and the second at ~230 K, which may be related to the narrowing of the main line. Taken together, this strongly suggests a two-step site transition. For example, before it has sufficient thermal energy to make the transition to the S site, the interstitial ^{8}Li may undergo thermally activated local dynamics, such as reorientation or partner exchange of a mixed interstitial configuration that nearly averages out the static quadrupolar splitting above about 70 K. At higher temperature, the (dynamic) interstitial makes the transition, as evident in $\lambda(T)$. Perhaps not coincidentally, this occurs at about the temperature of the onset of long-range vacancy diffusion in Nb (annealing stage III, 220 K).[45] In this scenario, the transition at 230 K is $V_{\mathrm{Nb}}+\mathrm{Li}_I^* \rightarrow \mathrm{Li}_{\mathrm{Nb}}$, where V_{Nb} denotes the host vacancy, and Li_I^* indicates the locally dynamic interstitial. We note that, at all temperatures, some of the implanted ^{8}Li becomes substitutional immediately. There is evidence for local defect dynamics preceding long-range diffusivity in metals.[46] For instance, motional averaging of the quadrupole splitting has been attributed to local jumping of implanted Fe atoms in the octahedral interstitial cage of an α-Zr host.[46,47] A similar phenomenon has been found for the implanted β-NMR probe ^{12}B in Si,[48] though there the impurity-host bonding is very different. In this dynamic interstitial model, the barrier obtained from the above two-site fit to $\lambda(T)$ of 900 K for a ν_a of 10^{12}/s corresponds to an activation energy for interstitial motion ~0.08 eV, similar to the activation energy for the local motion of Fe interstitials in α-Zr (0.07 eV) for an equivalent attempt frequency.[47] However, as previously stated, it is more realistic to expect a distribution of E_b (and possibly ν_a).

The spin-lattice relaxation of the dynamic interstitial contains a Korringa component, modified by dynamic averaging of the hyperfine coupling (yielding the lower slope at intermediate temperatures), as well as other relaxation mechanisms (magnetic or quadrupolar) connected with the motion itself, that would lead to the non-Korringa behavior, such as the negative intercept in the intermediate temperature region in Fig. 7. For example this is seen by β-NMR at the melting transition of bcc Li metal and its alloys, where a relaxation peak centered at T_m is superposed on the Korringa slope.[49] The peak in $\lambda(T)$ at about 220 K cannot be accounted for simply in this way, as it appears highly asymmetric with a long low-temperature tail. Further experiments at different fields and to higher temperatures are required to confirm the origin of the non-Korringa relaxation at intermediate temperatures. However, the data of Fig. 7 demonstrate the difficulty in making conclusions about metallicity based on non-Korringa behavior in $\lambda(T)$ over a restricted range of temperature.[50]

IV. SUMMARY

To summarize, we have studied the properties of implanted ^{8}Li in bcc Niobium to establish the behavior of the β-NMR probe as a prerequisite to study superconductivity in Nb films and heterostructures. We identified Li in two sites in

the lattice. At low temperature, the site is characterized by a well-defined quadrupolar splitting, but at relatively low-temperature ^{8}Li in this site becomes unstable. Close to room temperature, ^{8}Li makes a transition to the cubic substitutional site. The spin-lattice relaxation measurements are consistent with a site-dependent coupling to the Nb conduction electrons, but seem to include relaxation from another mechanism above 30 K. This picture of Li as an implanted interstitial at low temperature making the transition to substitutional at higher temperature is similar to fcc metals, such as Ag, Au, and Cu, but with the difference that the interstitial is distinguished by its quadrupolar splitting. Unlike the fcc metals, the site change seems to be a two-step process in Nb, reflecting the distinct defect properties of the bcc lattice.

This information may also be important in the interpretation of hyperfine fields in ferromagnetic bcc Fe.[51] A clear pattern is thus emerging for implanted ^{8}Li in metals: where ^{8}Li forms a defect with a weak, site-dependent coupling to the conduction band. Generally the interstitial site is metastable and more strongly coupled, having a higher Knight shift and a faster Korringa relaxation rate. The detailed site information may also be of interest in the application of Nb in proposed nuclear fusion reactors, where energetic Li implantation is expected.[37,52]

ACKNOWLEDGMENTS

We thank R. Abasalti, B. Hitti, M. Good, D. Arseneau, S. Daviel, and S. R. Kreitzman for technical assistance. We acknowledge NSERC Canada for funding and R. Liang and A. Lam for assistance with the x-ray characterization.

*Present address: LMU PSI, Villigen CH-5232, Switzerland.

[1] E. M. Forgan, S. J. Levett, P. G. Kealey, R. Cubitt, C. D. Dewhurst, and D. Fort, Phys. Rev. Lett. **88**, 167003 (2002); J. E. Sonier, M. F. Hundley, and J. D. Thompson, Phys. Rev. B **73**, 132504 (2006); A. Suter, E. Morenzoni, N. Garifianov, R. Khasanov, E. Kirk, H. Luetkens, T. Prokscha, and M. Horisberger, *ibid.* **72**, 024506 (2005).

[2] E.g., R. E. Laxdal, K. Fong, M. Laverty, A. Mitra, R. Poirier, I. Sekachev, and V. Zvyagintsev, Physica C **441**, 13 (2006).

[3] H. Tian, C. E. Reece, M. J. Kelley, S. Wang, L. Plucinski, K. E. Smith, and M. M. Nowell, Appl. Surf. Sci. **253**, 1236 (2006); A. T. Wu, Physica C **441**, 79 (2006); J. Halbritter, Appl. Phys. A: Mater. Sci. Process. **43**, 1 (1987).

[4] For NbO, T_C=1.5 K: W. W. Schulz, L. Forro, C. Kendziora, R. Wentzcovitch, D. Mandrus, L. Mihaly, and P. B. Allen, Phys. Rev. B **46**, 14001 (1992).

[5] I. Banerjee, Q. S. Yang, C. M. Falco, and I. K. Schuller, Solid State Commun. **41**, 805 (1982); W. P. Lowe and T. H. Geballe, Phys. Rev. B **29**, 4961 (1984).

[6] E.g., S. T. Ruggiero, T. W. Barbee, Jr., and M. R. Beasley, Phys. Rev. B **26**, 4894 (1982).

[7] M. Yudkowsky, W. P. Halperin, and I. K. Schuller, Phys. Rev. B **31**, 1637 (1985); R. H. Hammond and G. M. Kelly, Phys. Rev. Lett. **18**, 156 (1967); J. Lu, P. L. Kuhns, M. J. R. Hoch, W. G. Moulton, and A. P. Reyes, Phys. Rev. B **72**, 054401 (2005).

[8] G. D. Morris, W. A. MacFarlane, K. H. Chow, Z. Salman, D. J. Arseneau, S. Daviel, A. Hatakeyama, S. R. Kreitzman, C. D. P. Levy, R. Poutissou, R. H. Heffner, J. E. Elenewski, L. H. Greene, and R. F. Kiefl, Phys. Rev. Lett. **93**, 157601 (2004).

[9] Z. Salman, R. F. Kiefl, K. H. Chow, M. D. Hossain, T. A. Keeler, S. R. Kreitzman, C. D. P. Levy, R. I. Miller, T. J. Parolin, M. R. Pearson, H. Saadaoui, J. D. Schultz, M. Smadella, D. Wang, and W. A. MacFarlane, Phys. Rev. Lett. **96**, 147601 (2006).

[10] T. A. Keeler, Z. Salman, K. H. Chow, B. Heinrich, M. D. Hossian, B. Kardasz, R. F. Kiefl, S. R. Kreitzman, C. D. P. Levy, W. A. MacFarlane, O. Mosendz, T. J. Parolin, M. R. Pearson, and D. Wang, Phys. Rev. B **77**, 144429 (2008).

[11] T. J. Parolin, Z. Salman, K. H. Chow, Q. Song, J. Valiani, H. Saadaoui, A. O'Halloran, M. D. Hossain, T. A. Keeler, R. F. Kiefl, S. R. Kreitzman, C. D. P. Levy, R. I. Miller, G. D. Morris, M. R. Pearson, M. Smadella, D. Wang, M. Xu, and W. A. MacFarlane, Phys. Rev. B **77**, 214107 (2008).

[12] Z. Salman, A. I. Mansour, K. H. Chow, M. Beaudoin, I. Fan, J. Jung, T. A. Keeler, R. F. Kiefl, C. D. P. Levy, R. C. Ma, G. D. Morris, T. J. Parolin, D. Wang, and W. A. MacFarlane, Phys. Rev. B **75**, 073405 (2007).

[13] T. J. Parolin, Z. Salman, J. Chakhalian, Q. Song, K. H. Chow, M. D. Hossain, T. A. Keeler, R. F. Kiefl, S. R. Kreitzman, C. D. P. Levy, R. I. Miller, G. D. Morris, M. R. Pearson, H. Saadaoui, D. Wang, and W. A. MacFarlane, Phys. Rev. Lett. **98**, 047601 (2007).

[14] K. Mašek and V. Matolín, Thin Solid Films **317**, 183 (1998).

[15] A. R. Wildes, J. Mayer, and K. Theis-Bröhl, Thin Solid Films **401**, 7 (2001); G. Song, A. Remhof, K. Theis-Bröhl, and H. Zabel, Phys. Rev. Lett. **79**, 5062 (1997).

[16] C. D. P. Levy, A. Hatakeyama, Y. Hirayama, R. F. Kiefl, R. Baartman, J. A. Behr, H. Izumi, D. Melconian, G. D. Morris, R. Nussbaumer, M. Olivo, M. Pearson, R. Poutissou, and G. W. Wight, Nucl. Instrum. Methods Phys. Res. B **204**, 689 (2003).

[17] D. Borremans, D. L. Balabanski, K. Blaum, W. Geithner, S. Gheysen, P. Himpe, M. Kowalska, J. Lassen, P. Lievens, S. Mallion, R. Neugart, G. Neyens, N. Vermeulen, and D. Yordanov, Phys. Rev. C **72**, 044309 (2005).

[18] J. F. Ziegler, J. P. Biersack, and U. Littmark, *The Stopping and Range of Ions in Solids* (Pergamon, New York, 1985); SRIM is available at http://www.srim.org/

[19] W. A. MacFarlane, G. D. Morris, T. R. Beals, K. H. Chow, R. A. Baartman, S. Daviel, S. R. Dunsiger, A. Hatakeyama, S. R. Kreitzman, C. D. P. Levy, R. I. Miller, K. M. Nichol, R. Poutissou, and R. F. Kiefl, Physica B **326**, 213 (2003).

[20] T. Minamisono, T. Ohtsubo, I. Minami, S. Fukuda, A. Kitagawa, M. Fukuda, K. Matsuta, Y. Nojiri, S. Takeda, H. Sagawa, and H. Kitagawa, Phys. Rev. Lett. **69**, 2058 (1992).

[21] W. A. MacFarlane, G. D. Morris, K. H. Chow, R. A. Baartman, S. Daviel, S. R. Dunsiger, A. Hatakeyama, S. R. Kreitzman, C. D. P. Levy, R. I. Miller, K. M. Nichol, R. Poutissou, E. Dumont, L. H. Greene, and R. F. Kiefl, Physica B **326**, 209 (2003).

[22] M. Ogura and H. Akai, J. Phys. Condens. Matter **17**, 5741

(2005).
[23] D. N. Beshers, J. Appl. Phys. **36**, 290 (1965).
[24] T. Minamisono, Y. Nojiri, K. Asahi, and K. Ise, Hyperfine Interact. **15**, 547 (1983).
[25] B. Ittermann, K. Bürkmann, E. Diehl, R. Dippel, B. Fischer, H.-P. Frank, E. Jäger, W. Seelinger, G. Sulzer, H. Ackermann, and H.-J. Stöckmann, Z. Phys. B **91**, 7(1993).
[26] E.g., see the review, S. Hull, Rep. Prog. Phys. **67**, 1233 (2004).
[27] T. Minamisono, Y. Nojiri, and K. Matsuta, Phys. Lett. **94A**, 312 (1983).
[28] E. Jäger, B. Ittermann, H.-J. Stöckmann, K. Bürkmann, B. Fischer, H.-P. Frank, G. Sulzer, H. Ackermann, and P. Heitjans, Phys. Lett. A **123**, 39 (1987).
[29] A. Abragam, *Principles of Nuclear Magnetism* (Clarendon, Oxford, 1996).
[30] M. H. Cohen and F. Reif, in *Solid State Physics*, edited by F. Seitz and D. Turnbull (Academic, New York, 1957), Vol. 5, p. 321.
[31] M. L. Swanson, Vacuum **39**, 87 (1989); M. L. Swanson, L. M. Howe, and A. F. Quenneville, Nucl. Instrum. Methods **170**, 427 (1980).
[32] P. H. Dederichs, C. Lehmann, H. R. Scober, A. Scholz, and R. Zeller, J. Nucl. Mater. **69-70**, 176 (1978).
[33] P. Lucasson, P. Maury, and A. Lucasson, Radiat. Eff. **85**, 219 (1985).
[34] H. R. Paneth, Phys. Rev. **80**, 708 (1950); D. Nguyen-Manh, A. P. Horsfield, and S. L. Dudarev, Phys. Rev. B **73**, 020101(R) (2006).
[35] H. Metzner, R. Sielemann, S. Klaumünzer, R. Butt, and W. Semmler, Z. Phys. B **61**, 267 (1985).
[36] P. M. Derlet, D. Nguyen-Manh, and S. L. Dudarev, Phys. Rev. B **76**, 054107 (2007).
[37] J. Rottler, D. J. Srolovitz, and R. Car, Phys. Rev. B **71**, 064109 (2005).
[38] M. Xu, M. D. Hossain, H. Saadaoui, T. J. Parolin, K. H. Chow, T. A. Keeler, R. F. Kiefl, G. D. Morris, Z. Salman, Q. Song, D. Wang, and W. A. MacFarlane, J. Magn. Reson. **191**, 47 (2008).
[39] J. Xue, Q. Zhou, H. Suzuki, and S. Misawa, J. Low Temp. Phys. **121**, 127 (2000); D. Hechtfischer, Z. Phys. B **23**, 255 (1976).
[40] C. P. Slichter, *Principles of Magnetic Resonance*, 3rd ed. (Springer-Verlag, Berlin, 1990).
[41] M. D. Hossain, Z. Salman, D. Wang, K. H. Chow, S. Kreitzman, T. A. Keeler, C. D. P. Levy, W. A. MacFarlane, R. I. Miller, G. D. Morris, T. J. Parolin, M. Pearson, H. Saadaoui, and R. F. Kiefl, Phys. Rev. B **79**, 144518 (2009).
[42] M. D. Hossain, H. Saadaoui, T. J. Parolin, Q. Song, D. Wang, M. Smadella, K. H. Chow, M. Egilmez, I. Fan, R. F. Kiefl, S. R. Kreitzman, C. D. P. Levy, G. D. Morris, M. R. Pearson, Z. Salman, and W. A. MacFarlane, Physica B **404**, 914 (2009).
[43] G. C. Carter, L. H. Bennett, and D. J. Kahan, in *Metallic Shifts in NMR, Progress in Materials Science*, edited by B. Chalmers, J. W. Christian, and T. B. Massalski (Pergamon Press, Oxford, 1977), Vol. 20.
[44] B. S. Shastry and E. Abrahams, Phys. Rev. Lett. **72**, 1933 (1994).
[45] P. Ehrhart and H. Schultz, in *Atomic Defects in Metals*, edited by H. Ullmaier, Landolt-Börnstein, New Series, Group III, Vol. 25, Condensed Matter (Springer-Verlag, Heidelberg, 1991) Chap. 2.
[46] G. Vogl, Phys. Status Solidi B **144**, 259 (1987).
[47] Y. Yoshida, M. Menningen, R. Sielemann, G. Vogl, G. Weyer, and K. Schröder, Phys. Rev. Lett. **61**, 195 (1988).
[48] R. E. McDonald, T. K. McNab, J. A. Becker, J. D. Perez, Hyperfine Interact. **4**, 782 (1978); H.-P. Frank, T. Almeida, E. Diehl, K.-H. Ergezinger, B. Fischer, B. Ittermann, F. Mai, W. Seelinger, S. Weissenmayer, G. Welker, H. Ackermann, and H.-J. Stöckmann, *ibid.* **79** 655–658 (1993); B. Ittermann, D. Peters, M. Füllgrabe, F. Kroll, H. Ackermann, and H.-J. Stöckmann, Physica B **308-310**, 236 (2001).
[49] A. Korblein, P. Heitjans, H.-J. Stockmann, F. Fujara, H. Ackermann, W. Buttler, K. Dorr and, H. Grupp, J. Phys. F: Met. Phys. **15**, 561 (1985).
[50] E.g., C. Weindel, H. J. Jänsch, G. Kirchner, J. J. Paggel, H. Winnefeld, and D. Fick, Phys. Rev. B **72**, 033307 (2005).
[51] N. Severijns, J. Wouters, J. Vanhaverbeke, W. Vanderpoorten, and L. Vanneste, Hyperfine Interact. **60**, 889 (1990); K. Matsuta, M. Sasaki, T. Tsubota, S. Kaminaka, K. Hashimoto, S. Kudo, M. Ogura, K. Arimura, M. Mihara, M. Fukuda, H. Akai, and T. Minamisono, *ibid.* **136-137**, 379 (2001).
[52] J. P. Biersack and D. Fink, J. Nucl. Mater. **53**, 328 (1974); F. K. Altenhein, H. Andresen, W. Lutze, G. Malow and H. Migge, *ibid.* **53**, 332 (1974).